Am J Transl Res 2026;18(11):9680-9695
www.ajtr.org /ISSN:1943-8141/AJTR0174549

Original Article

Guizhi-Shaoyao-Zhimu Decoction alleviates rheumatoid arthritis by upregulating lncRNA GAS5 and suppressing PI3K/Akt phosphorylation

Zhiqiang Wang[1,2], Xing Feng[1], Yajing Wang[1], Zhenbin Li[1,2]

[1]*Department of Rheumatology and Clinical Immunology, No. 980 Hospital of The Joint Logistics Support Force, Shijiazhuang, Hebei, China;* [2]*The First Clinical Medical College of Nanjing University of Chinese Medicine, Nanjing, Jiangsu, China*

Received June 6, 2026; Accepted September 7, 2026; Epub November 15, 2026; Published November 30, 2026

Abstract: Objectives: To evaluate the clinical efficacy of Guizhi-Shaoyao-Zhimu Decoction (GSZD) in rheumatoid arthritis (RA) and to explore whether it acts through the lncRNA GAS5/PI3K/Akt axis. Methods: A retrospective study was conducted on 60 RA patients (30 received methotrexate (MTX) alone, 30 received MTX+GSZD) for 12 weeks. Clinical symptoms, inflammatory markers, disease activity scores (DAS28-ESR, DAS28-CRP), and TCM symptom scores were assessed. An in vivo CIA rat model was used to evaluate joint inflammation and histopathology. Network pharmacology and molecular docking were performed to predict active components and targets. In vitro, TNF-α-stimulated MH7A cells were treated with GSZD, and lncRNA GAS5 expression, viability, apoptosis, and PI3K/Akt phosphorylation were measured. Rescue experiments used shRNA to knock down lncRNA GAS5. Results: GSZD+MTX significantly reduced swollen joint count (SJC), Visual Analogue Scale (VAS), DAS28-ESR, DAS28-CRP, TNF-α, and IL-6 compared with MTX alone ($P < 0.01$), improved TCM symptom scores ($P < 0.0001$), and achieved a 96.7% effective rate vs. 20.0% ($P < 0.0001$). In CIA rats, GSZD dose-dependently reduced arthritis index and paw swelling, and alleviated synovial hyperplasia, inflammatory infiltration, and cartilage erosion. Network pharmacology identified 201 active ingredients (e.g., quercetin, kaempferol, luteolin) and 7 core targets (AKT1, IL6, TNF, TP53, IL1B, PTGS2, ESR1), with PI3K/Akt as a key pathway. In MH7A cells, GSZD reversed TNF-α-induced GAS5 downregulation ($P < 0.001$), suppressed viability, promoted apoptosis, and inhibited PI3K/Akt phosphorylation; GAS5 knockdown abolished these effects. Conclusions: GSZD is associated with improved clinical outcomes and alleviates CIA in rats. Its mechanism involves upregulating lncRNA GAS5 and inhibiting PI3K/Akt signaling, providing an epigenetic basis for GSZD in RA.

Keywords: Guizhi-Shaoyao-Zhimu Decoction, rheumatoid arthritis, lncRNA GAS5, PI3K/Akt, network pharmacology, fibroblast-like synoviocytes

Introduction

Rheumatoid arthritis (RA) is a systemic autoimmune disease characterized by chronic synovial inflammation and progressive joint destruction. Its global prevalence is approximately 0.5%-1%. RA can lead to joint deformity, functional loss, and damage to multiple organs throughout the body, imposing a substantial burden on patients and healthcare systems [1]. The pathological core of RA lies in the abnormal activation and proliferation of fibroblast-like synoviocytes (FLS) in the synovial tissue. These cells secrete large amounts of pro-inflammatory cytokines (e.g., tumor necrosis factor-α (TNF-α), interleukin-6 (IL-6)) and matrix metalloproteinases (MMPs), directly driving synovial inflammation, pannus formation, and erosive destruction of cartilage and bone [2]. Although disease-modifying antirheumatic drugs such as methotrexate (MTX) and biological agents have significantly improved the treatment outcomes of RA, a considerable proportion of patients still have poor responses or adverse reactions, and are prone to relapse after discontinuation. Therefore, exploring new and safer effective treatment strategies remains an important direction in RA research.

https://doi.org/10.62347/CBDR1882

Traditional Chinese medicine has a long history of experience in RA treatment, emphasizing holistic regulation and syndrome differentiation. Guizhi-Shaoyao-Zhimu Decoction (GSZD), derived from Zhang Zhongjing's Jin Kui Yao Lue, consists of nine herbs: Cinnamomi Ramulus (Guizhi), Paeoniae Radix Alba (Baishao), Anemarrhenae Rhizoma (Zhimu), Ephedrae Herba (Mahuang), Saposhnikoviae Radix (Fangfeng), Atractylodis Macrocephalae Rhizoma (Baizhu), Aconiti Lateralis Radix Praeparata (Fuzi), Zingiberis Rhizoma Recens (Shengjiang), and Glycyrrhizae Radix et Rhizoma (Gancao). It is a classic prescription for RA of the cold-dampness obstruction type. Clinical studies have shown that GSZD combined with conventional Western medicine can significantly reduce joint swelling and pain in RA patients, and patients experience fewer adverse reactions [2]. Animal experiments have confirmed that GSZD can alleviate joint inflammation and bone destruction in collagen-induced arthritis (CIA) rats and inhibit abnormal proliferation and invasion of FLS [3]. However, the molecular mechanism of GSZD in anti-RA has not been fully elucidated, especially whether it acts through epigenetic regulation, and there is still a lack of in-depth research.

Long non-coding RNA (lncRNA) growth arrest-specific transcript 5 (GAS5) is a recently identified molecule with tumor-suppressive and anti-inflammatory functions. Studies have found that the expression of lncRNA GAS5 in peripheral blood mononuclear cells and synovial tissues of RA patients is significantly downregulated, and its level is negatively correlated with disease activity [4]. Serum levels of GAS5 are also decreased in RA patients [5]. Mechanistically, lncRNA GAS5 can regulate downstream key pathways through competitive endogenous RNA (ceRNA) mechanisms or direct binding to signaling proteins. Among them, the PI3K/Akt signaling axis is a well-recognized downstream target of GAS5: lncRNA GAS5 can negatively regulate the PI3K/Akt pathway through multiple mechanisms, including sponging microRNAs such as miR-21, thereby inhibiting abnormal cell proliferation and inflammatory responses [6]. For instance, Yang et al. demonstrated that lncRNA GAS5 alleviates RA by sponging miR-222-3p to upregulate Sirt1, thereby suppressing FLS proliferation and inflammatory responses [5]. The abnormal activation of the PI3K/Akt pathway plays a core role in the proliferation, migration, invasion, and anti-apoptosis of RA-FLS, and serves as a key crosstalk node between FLS and osteoclasts, targeting this pathway has been shown to be a potential strategy for RA treatment [7]. However, whether GSZD can affect the PI3K/Akt axis by regulating lncRNA GAS5 and thereby inhibit the malignant phenotype of RA-FLS and reduce synovial inflammation and joint destruction has not been reported.

Based on the above background, this study proposes a scientific hypothesis: GSZD may increase lncRNA GAS5 expression, thereby inhibiting the PI3K/Akt signaling pathway and consequently suppressing the abnormal activation of RA-FLS, reducing synovial inflammation and joint destruction. To verify this hypothesis, this study adopts a multi-level experimental design: first, through clinical case observation (comparing the efficacy of MTX alone and MTX combined with GSZD) to clarify the clinical value of GSZD; second, using the CIA rat model to verify the anti-inflammatory and joint protection effects of GSZD in vivo; third, through network pharmacology and molecular docking to predict the core targets and key pathways of GSZD in treating RA; finally, in the TNF-α-induced MH7A cell (human RA-FLS cell line) model, through shRNA-mediated knockdown of lncRNA GAS5, to verify in reverse whether GSZD exerts its anti-proliferation, pro-apoptosis, and anti-inflammatory effects through the lncRNA GAS5/PI3K/Akt axis. This study aims to reveal the molecular mechanism of GSZD in treating RA from a new perspective of epigenetic regulation and provide a more solid experimental basis for its clinical application.

Materials and methods

Clinical data

Study subjects: Patients with RA who visited the Department of Rheumatology and Immunology at No. 980 Hospital of the Joint Logistics Support Force from January 2021 to December 2023 were included. They were divided into two groups based on whether they received Guizhi Shaoyao Zhimu Decoction (GSZD) treatment: the control group (treated

with methotrexate alone) had 30 cases, and the treatment group (treated with methotrexate + GSZD) had 30 cases. This study was conducted in accordance with the Declaration of Helsinki (as revised in 2013) and was approved by the Ethics Committee of No. 980 Hospital of the Joint Logistics Support Force (Approval No. 2023-KY-74. All patients provided written informed consent. Initially, 64 patients with RA were enrolled. During the 12-week treatment period, four patients dropped out: two in the control group (MTX alone) due to elevated liver enzymes, and two in the treatment group (MTX + GSZD) due to intolerance to the decoction. Ultimately, 60 patients (30 in each group) completed the study and were included in the final analysis.

Diagnostic criteria: Western Medicine Diagnostic Criteria: RA was diagnosed based on the 2010 American College of Rheumatology (ACR) and the European League Against Rheumatism (EULAR).

Traditional Chinese Medicine Diagnostic Criteria: According to the "Diagnosis and Treatment Guidelines for Rheumatoid Arthritis Based on Syndrome Combination" of the Rheumatology Branch of the Chinese Association of Traditional Chinese Medicine, patients who met the diagnostic criteria of the cold-dampness obstruction syndrome of RA. Main symptoms: (1) Cold pain in the joints, not warm upon palpation, no redness of the skin; (2) Pain worsens with cold and relieves with heat. Secondary symptoms: (1) Joint stiffness, limited flexion and extension; (2) Cold limbs, or preferring warmth; (3) Tasteless mouth and no thirst. Tongue and pulse: Enlarged tongue body, pale tongue quality, white or greasy coating, stringy or tight pulse.

Inclusion and exclusion criteria: Inclusion criteria: (1) Meet the Western medicine classification criteria for RA; (2) Meet the diagnostic criteria for the cold-dampness obstruction syndrome of RA according to the "Diagnosis and Treatment Guidelines for Rheumatoid Arthritis Based on Syndrome Combination" of the Rheumatology Branch of the Chinese Association of Traditional Chinese Medicine; (3) Age 18-70 years old, gender not limited; (4) 28-joint Disease Activity Score (DAS28-ESR) > 2.6 based on ESR.

Exclusion criteria: (1) Patients diagnosed with or with overlap of other connective tissue diseases; (2) Those who had received glucocorticoid treatment within the previous 12 weeks; (3) Those who have received other csDMARDs, bDMARDs, or tsDMARDs; (4) Pregnant or lactating women; (5) Patients with allergic constitution or a severe history of medication allergy; (6) Those with severe diseases in the cardiovascular, nervous, and blood systems; (7) Those who could not cooperate with treatment; (8) Those with poor compliance.

Treatment: Both groups received methotrexate (MTX) 10-15 mg once weekly, and folic acid 10 mg was taken orally on the day after MTX administration. Concomitant use of stable-dose of non-steroidal anti-inflammatory drugs (NSAIDs) was permitted; other medications not interfering with the study treatment were also allowed. On the basis of this treatment, the treatment group additionally received Guizhi-Shaoyao-Zhimu Decoction (GSZD) consisting of Cinnamomi Ramulus (Guizhi) 12 g, Paeoniae Radix Alba (Baishao) 9 g, Ephedrae Herba (Mahuang) 6 g, Zingiberis Rhizoma Recens (Shengjiang) 15 g, Atractylodis Macrocephalae Rhizoma (Baizhu) 15 g, Anemarrhenae Rhizoma (Zhimu) 9 g, Saposhnikoviae Radix (Fangfeng) 12 g, Aconiti Lateralis Radix Praeparata (Fuzi) 6 g, and Glycyrrhizae Radix et Rhizoma (Gancao) 6 g. The decoction was taken once daily, divided into morning and evening doses. Both groups were treated continuously for 12 weeks.

Observation indicators: Conventional clinical indicators: Number of tender joints (TJC), number of swollen joints (SJC), Visual Analogue Scale (VAS), erythrocyte sedimentation rate (ESR), C-reactive protein (CRP), tumor necrosis factor-α (TNF-α), interleukin-6 (IL-6), DAS28-ESR, DAS28-CRP.

Traditional Chinese Medicine Indicators: Refer to the quantification table for evaluating TCM symptoms in the "Guidelines for Clinical Research of New Traditional Chinese Medicines" in 2002, assess the single-item scores and total scores of joint pain, joint swelling, joint tenderness, limited flexion and extension, cold sensation of the joint, aversion to cold and wind, cold limbs, coldness and lack of warmth in the limbs, soreness of the waist and knees, morning stiffness, etc. TCM symptom score

improvement rate = (pre-treatment score - post-treatment score)/pre-treatment score × 100%. Efficacy determination criteria: Clinical remission (improvement rate ≥ 70%), marked improvement (50% ≤ improvement rate < 70%), effective (20% ≤ improvement rate < 50%), ineffective (improvement rate < 20%). Total effective rate = (number of clinical remission + marked improvement + effective cases)/total cases × 100%.

Animal experiments

Experimental animals: Seventy SPF-grade Wistar rats, aged 42-55 days, weighing 230-260 g, were purchased from Beijing Vitogen Laboratory Animal Technology Co., Ltd. [Production License Number: SCXK (Jing) 2016-0006]. They were housed in the animal room of the experimental center, with a room temperature of 23 ± 2°C, humidity of 55 ± 2%, 12-h light/12-h dark cycle, and free access to food and water. All animal procedures were approved by the Animal Ethics Committee of No. 980 Hospital of the Joint Logistics Support Force (Approval No. 2023-KY-74) and were performed in accordance with the National Institutes of Health Guide for the Care and Use of Laboratory Animals. The 70 Wistar rats were purchased for a series of experiments within the same approved project; 24 rats were used for the formal experiment and 46 were allocated to preliminary model validation and dose-finding studies. After completion of all experiments, all animals were euthanized by intraperitoneal injection of sodium pentobarbital (80 mg/kg), followed by cervical dislocation to ensure death, in accordance with the AVMA Guidelines for the Euthanasia of Animals. All efforts were made to minimize suffering and reduce the number of animals used.

Drug preparation: GSZD was composed of Cinnamomi Ramulus (Guizhi) 12 g, Paeoniae Radix Alba (Baishao) 9 g, Ephedrae Herba (Mahuang) 6 g, Zingiberis Rhizoma Recens (Shengjiang) 15 g, Atractylodis Macrocephalae Rhizoma (Baizhu) 15 g, Anemarrhenae Rhizoma (Zhimu) 9 g, Saposhnikoviae Radix (Fangfeng) 12 g, Aconiti Lateralis Radix Praeparata (Fuzi) 6 g, and Glycyrrhizae Radix et Rhizoma (Gancao) 6 g. The herbal pieces were soaked in 500 mL water for 30 min, boiled for 30 min, and filtered; the residue was re-extracted with 500 mL of water for 30 min and filtered. The two filtrates were combined and concentrated to 200 mL. Low and high doses were set as 800 mg and 3,200 mg of crude drug per kg of body weight, respectively. The high dose was prepared from the original concentrate, and the low dose was obtained by a 4-fold dilution with pure water.

Establishment of CIA rat model: Bovine type II collagen (CII) was dissolved in pre-cooled 0.05 mol/L acetic acid solution to prepare a 2 mg/mL solution. The next day, an equal volume of CII solution was mixed with Freund's complete adjuvant (CFA) under ice bath conditions, and vortexed to emulsify. The emulsification was confirmed by the drop-test in cold water. Primary immunization: Multiple intradermal injections of 200 μL emulsified liquid were made at the tail root of the rats. The second booster immunization was performed on the 21st day, with 100 μL emulsified liquid injected. An AI score of ≥ 4 indicated successful modeling.

Animal grouping and intervention: The rats were randomly divided into 4 groups, with 6 rats in each group: (1) Normal control group (without CIA induction, receiving equal volume of distilled water by gavage); (2) CIA model group (CIA induction + equal volume of distilled water by gavage); (3) GSZD low-dose group (CIA induction + 800 mg/kg GSZD by gavage); (4) GSZD high-dose group (CIA induction + 3200 mg/kg GSZD by gavage). Gavage administration began the day after the second immunization, once daily, for 14 consecutive days.

Assessment of joint inflammation: AI score: 0 points (no redness or swelling), 1 point (redness of individual toes), 2 points (significantly red footpad), 3 points (swelling of the ankle joint), 4 points (severe redness of ankle and entire foot). The sum of limb scores was the final AI (maximum 16 points). The degree of foot swelling in the hind limb: Mark the right hind tarsal bone protrusion, measure the circumference of the most swollen part of the foot with a soft thin string, accurate to 0.1 mm. AI was evaluated once a day, and the foot circumference was evaluated once a week.

Histopathological examination of ankle joint tissue: After the experiment, the rat ankle joints were taken, fixed in 4% paraformaldehyde

for 48 hours, rinsed with running water for 60 minutes. After gradient ethanol dehydration, xylene transparency, and paraffin embedding, 4 μm-thick sections were cut. HE staining: Dehydration, hydration, hematoxylin staining for 10 minutes, and eosin staining for 2 minutes. Gradient dehydration, transparency, and neutral gum mounting occured, followed by observation under an optical microscope.

Network pharmacology analysis: Screening of active components and targets of GSZD.

All active components of the 9 herbs in GSZD were searched in the TCMSP database. Candidate active components were selected based on oral bioavailability (OB) ≥ 30% and drug-likeness (DL) ≥ 0.18. The action targets of the candidate components were retrieved in TCMSP and standardized using the UniProt database, and duplicate targets were eliminated.

Collection of RA disease targets: RA-related disease targets were retrieved from DisGeNET, DrugBank, GeneCards, OMIM, pharmGKB, and TTD databases, using the keyword "rheumatoid arthritis". Duplicates were excluded.

Network construction and analysis: The intersection of GSZD's active targets and RA disease targets was used to draw a Venn diagram. The "GSZD-Medicine-Active Component-Target-RA" network was constructed using Cytoscape 3.8.2 software, and the main active components were selected based on the degree value. The intersecting targets were input into the STRING 12.0 platform to construct a protein-protein interaction (PPI) network, with the species set as "Homo sapiens". Topological analysis was performed using the cytoHubba plugin, and the top 10 intersecting targets ranked by degree, MCC, Closeness, and Betweenness were selected to obtain the core targets.

Molecular docking: The top 3 active components (quercetin, kaempferol, luteolin) with the highest degree values were selected as ligands, and the core targets of the PPI network (AKT1, IL6, TNF, TP53, IL1B, PTGS2, ESR1) were selected as receptors. The 3D structures were downloaded from PubChem and RCSB databases, and imported into the CB-DOCK2 platform for molecular docking. The position with the lowest binding energy (Vina score) was selected as the best docking mode. A binding energy < -5.0 kcal/mol indicated good binding activity.

Quality control of GSZD: The chemical profile of GSZD has been well characterized in previous studies. A validated HPLC fingerprint method established for GSZD identified 26 common peaks with a similarity range of 0.929-0.998 across different batches, and eight major components (including mangiferin, paeoniflorin, glycyrrhizin, and others) were assigned [8]. The GSZD decoction used in this study was prepared following the same protocol as reported, ensuring batch-to-batch consistency.

Cell experiments

Cell source and culture: The human synovial fibroblast cell line MH7A (verified by STR and negative for mycoplasma) was cultured in DMEM high-glucose complete medium containing 10% fetal bovine serum and 1% penicillin-streptomycin. Cells were cultured in a 37°C, 5% CO_2, saturated humidity incubator. When confluence reached 80%-90%, cells were digested and passaged with 0.25% trypsin-EDTA.

Drug treatment and grouping: The GSZD freeze-dried powder (prepared by decocting the above traditional Chinese medicine decoction pieces and freeze-drying) was dissolved in complete medium. After inoculation, cells were cultured until the confluence was approximately 80%, media was then replaced with serum-free medium for synchronization for 6 hours. Preliminary CCK-8 assays showed no significant cytotoxicity at concentrations up to 1,000 μg/mL; therefore, 1,000 μg/mL GSZD was used in subsequent experiments. Experimental grouping: (1) Blank control group (0.1% DMSO); (2) TNF-α group (stimulated with 10 ng/mL TNF-α for 24 h); (3) GSZD + TNF-α group (1,000 μg/mL GSZD pretreated for 30 min followed by addition of 10 ng/mL TNF-α for co-culture for 24 h).

Cell transfection (shRNA knockdown): Using Lipofectamine 3,000 reagent, the shRNA expression plasmid targeting lncRNA GAS5 (sh-lncRNA GAS5 1#, 2#, 3#) or negative control plasmid (sh-NC) was transfected into MH7A

Table 1. Baseline characteristics of patients in the two groups

Group	Control (n = 30)	Treatment (n = 30)	t/χ^2	P
Sex (male/female) (n)	8/22	9/21	0.082	0.775
Age (years)	41.77 ± 13.70	42.97 ± 11.62	0.366	0.716
ESR (mm/h)	51.07 ± 18.38	55.37 ± 21.58	0.831	0.409
CRP (mg/L)	40.13 ± 17.22	47.37 ± 19.56	1.523	0.133
DAS28-ESR	5.89 ± 0.65	6.02 ± 0.51	0.888	0.378
DAS28-CRP	5.45 ± 0.55	5.587 ± 0.47	1.076	0.287
TCM symptom score	41.30 ± 6.43	45.00 ± 6.78	2.169	0.064
TNF-α	31.50 ± 10.20	30.20 ± 9.80	0.503	0.617
IL-6	35.50 ± 16.50	35.00 ± 16.00	0.119	0.906

Abbreviation: ESR, erythrocyte sedimentation rate; CRP, C-reactive protein; DAS28-ESR, Disease Activity Score in 28 joints based on erythrocyte sedimentation rate; DAS28-CRP, Disease Activity Score in 28 joints based on C-reactive protein; TCM, Traditional Chinese Medicine; TNF-α, tumor necrosis factor-α; IL-6, interleukin-6; SD, standard deviation.

cells. Forty-eight hours after transfection, the knockdown efficiency was verified by qPCR.

Real-time fluorescence quantitative PCR (qPCR): Total RNA was extracted using the TRIzol method, purity was detected (A260/A280 1.8-2.1) with NanoDrop. cDNA was reverse transcribed using PrimeScript RT Master Mix, and amplified using SYBR Premix Ex Taq II on qPCR instrument. The expression of lncRNA GAS5 was detected with β-actin as the internal reference. The relative expression level was calculated using the 2-ΔΔCt method.

Cell viability detection (CCK-8): Cells were inoculated into 96-well plates, treated according to the grouping, with 10 μL CCK-8 reagent added to each well. They were then, incubated at 37°C in the dark for 1-2 hours, and the absorbance was measured at 450 nm using an enzyme detector. The relative viability of cells = (experimental group OD value/control group OD value) × 100%.

Flow cytometry detection of apoptosis: Cells were collected, digested with EDTA-free trypsin, and washed with PBS. They were then resuspend with 100 μL 1× Annexin V binding buffer, mixed with 5 μL Annexin V-FITC and 5 μL PI, incubated at room temperature in the dark for 15 minutes, given 400 μL binding buffer, and detected within 1 hour using a flow cytometer. The total apoptosis rate is the sum of early apoptosis (Annexin V+/PI-) and late apoptosis (Annexin V+/PI+).

Western blot: Total protein was extracted using RIPA lysis buffer (containing PMSF, proteinase inhibitor, and phosphatase inhibitor), quantify with BCA method. After SDS-PAGE electrophoresis of protein samples, protein was transfered to PVDF membrane, 5% BSA blocking for 2 hours. Membranes were incubated with primary antibodies (p-PI3K, PI3K, p-Akt, Akt, β-actin) at 4°C overnight, then with secondary antibody at room temperature for 2 h, and signals were detected using ECL. Bands were analyzed using the gray value with Image J software, and the phosphorylation level of target protein was expressed as the ratio of phosphorylation to total protein.

Statistical analysis

Data were analyzed using GraphPad Prism 9.0 software. Continuous variables are expressed as mean ± standard deviation (Mean ± SD). Normality was assessed using the Shapiro-Wilk test. For comparisons between two groups, the two-tailed Student's t-test was used. For multiple group comparisons, one-way analysis of variance (ANOVA) was performed followed by Tukey's post hoc test for multiple comparison correction. Categorical data were analyzed using the χ^2 test. A P value < 0.05 was considered statistically significant. All cell experiments were repeated at least three independent times.

Results

Clinical efficacy comparison

Of the 64 initially enrolled patients, 4 discontinued treatment (2 in the control group due to elevated liver enzymes, and 2 in the treatment group due to intolerance to the decoction). The remaining 60 patients (30 in each group) were included in the final analysis. Baseline characteristics were comparable between the two groups (**Table 1**). They were divided into the control group (treated with methotrexate alone, 30 cases) and the treatment group (treated with methotrexate + GSZD, 30 cases) based on

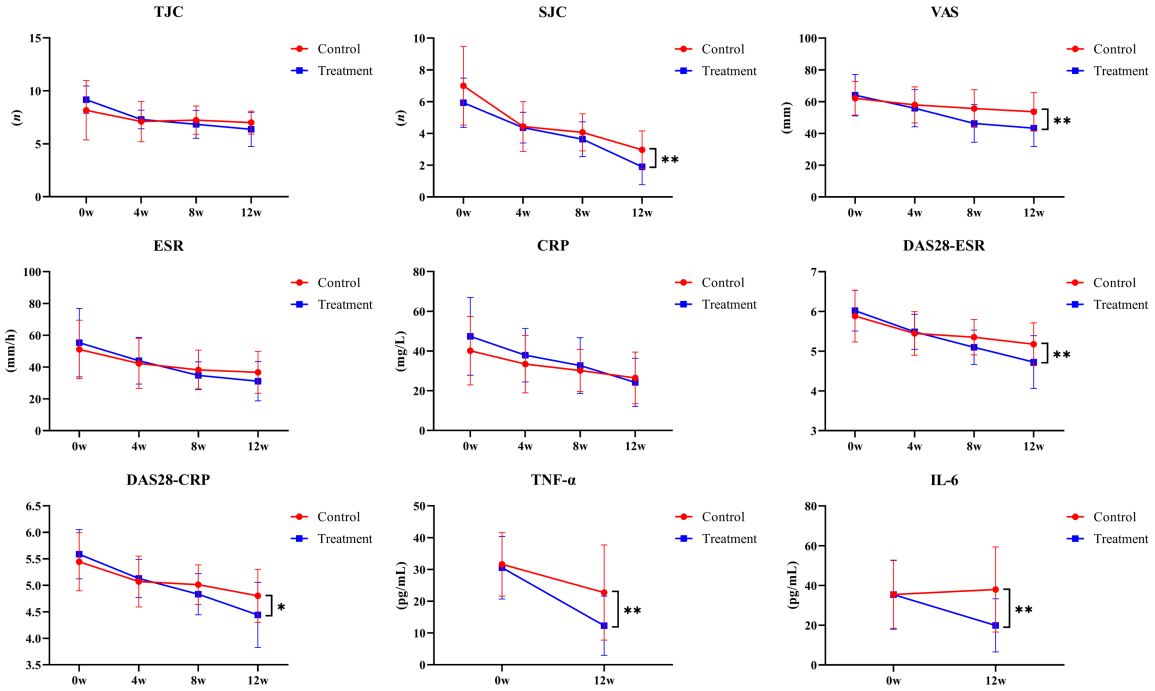


Figure 1. Comparison of Western medicine indicators between the two groups before and after treatment. Data are presented as mean ± SD (n = 30 per group). $^{**}P < 0.01$ vs. control group. Abbreviation: TJC, tender joint count; SJC, swollen joint count; VAS, Visual Analogue Scale; ESR, erythrocyte sedimentation rate; CRP, C-reactive protein; DAS28-ESR, Disease Activity Score in 28 joints based on erythrocyte sedimentation rate; DAS28-CRP, Disease Activity Score in 28 joints based on C-reactive protein; TNF-α, tumor necrosis factor-α; IL-6, interleukin-6.

Table 2. Post-treatment clinical indicators at week 12

Indicator	Control (mean ± SD)	Treatment (mean ± SD)	t	*P*-value
TJC (n)	5.21 ± 2.24	4.53 ± 2.11	0.892	0.376
ESR (mm/h)	25.00 ± 10.13	22.11 ± 9.67	1.160	0.250
CRP (mg/L)	20.00 ± 8.26	18.01 ± 7.84	0.977	0.332
SJC (n)	6.52 ± 2.41	3.22 ± 1.83	6.310	< 0.001
VAS (mm)	45.01 ± 11.72	25.00 ± 10.84	6.804	< 0.001
DAS28-ESR	5.20 ± 0.79	3.23 ± 0.71	9.241	< 0.001
DAS28-CRP	4.50 ± 0.74	2.80 ± 0.66	9.440	< 0.001
TNF-α (pg/mL)	30.03 ± 12.75	15.05 ± 10.42	4.946	< 0.001
IL-6 (pg/mL)	50.03 ± 14.61	20.11 ± 12.28	8.615	< 0.001

Abbreviation: TJC, tender joint count; ESR, erythrocyte sedimentation rate; CRP, C-reactive protein; SJC, swollen joint count; VAS, Visual Analogue Scale; DAS28-ESR, Disease Activity Score in 28 joints based on erythrocyte sedimentation rate; DAS28-CRP, Disease Activity Score in 28 joints based on C-reactive protein; TNF-α, tumor necrosis factor-α; IL-6, interleukin-6; SD, standard deviation.

whether they received the treatment of Guizhi Shaoyao Zhimu Decoction (GSZD). There were no statistically significant differences in baseline data (gender, age, ESR, CRP, DAS28-ESR, DAS28-CRP, and TCM symptom scores) between the two groups ($P > 0.05$, **Table 1**), thus they were comparable. After treatment, the treatment group had significantly lower swollen joint count (SJC), visual analogue scale (VAS), DAS28-ESR, DAS28-CRP, tumor necrosis factor-α (TNF-α), and interleukin-6 (IL-6) compared to the control group ($P < 0.01$, **Figure 1**; **Table 2**). For TJC, ESR, and CRP, both groups improved from baseline, but the intergroup differences were not statistically significant ($P > 0.05$, **Figure 1**; **Table 2**). After treatment, the TCM symptom scores of the treatment group were significantly lower than those of the control group ($P < 0.0001$), and the improvement degree of TCM symptom scores was also significantly better than that of the control group ($P < 0.0001$, **Figure 2A**, **2B**). In terms of individual TCM symptoms, the scores of the treatment group in joint tenderness, limited movement, cold sensation of the joint, aversion to wind and cold, cold extremities, soreness of the waist

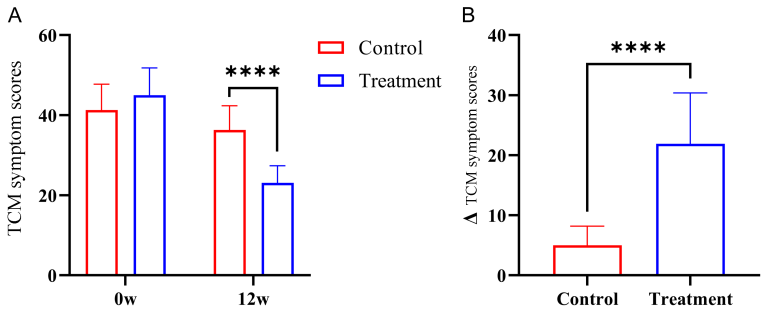


Figure 2. Comparison of TCM symptom scores between the two groups. A. TCM symptom scores before and after treatment; B. Improvement rate of TCM symptom scores. Data are presented as mean ± SD (n = 30 per group). ****P < 0.0001 vs. control group. Abbreviation: TCM, Traditional Chinese Medicine.

and knees, and morning stiffness were significantly lower than those of the control group (P < 0.01). The TCM efficacy evaluation showed that the total effective rate of the treatment group was 96.7% (29/30), including 1 case of clinical remission, 16 cases of marked improvement, and 12 cases of effective improvement; the total effective rate of the control group was 20.0% (6/30), with no cases of clinical remission or marked improvement. The difference in total effective rate between the two groups was statistically significant (P < 0.0001, **Table 3**).

Animal experiment results

In the collagen-induced arthritis (CIA) rat model, compared with the CIA model group, the AI score and paw circumference in the low- and high-dose GSZD groups significantly decreased from the middle to later stages of treatment (P < 0.05 or P < 0.001), and the dose-dependent effect was observed. The improvement effect of the high-dose GSZD group was the most significant (**Figure 3**). The results of HE staining showed that the ankle joint structure of the normal control group rats was intact, the synovium was thin and continuous, and there was no inflammatory cell infiltration. The CIA model group showed typical RA pathological changes: significant synovial hyperplasia, narrowed joint cavity, massive inflammatory cell infiltration, pannus formation, and erosion of the cartilage surface. After GSZD intervention, the above pathological changes were improved to varying degrees, and the joint structure of the high-dose group was basically normal, with a significant reduction in the range of synovial hyperplasia and inflammatory infiltration (**Figure 4**).

Network pharmacology analysis results

After screening with oral bioavailability (OB) ≥ 30% and drug-likeness (DL) ≥ 0.18, 201 candidate active ingredients were obtained from the 9 Chinese herbal medicines of GSZD (**Table 4**), corresponding to 264 target sites. Intersecting with 6,989 RA-related targets, 204 potential targets for GSZD treatment of RA were obtained. Protein-protein interaction (PPI) network topological analysis screened out 7 core targets: AKT1, IL6, TNF, TP53, IL1B, PTGS2, ESR1 (**Table 5**). Molecular docking results showed that the binding energies of the main active ingredients quercetin, kaempferol, and luteolin with the above core target proteins were all less than -5.0 kcal/mol, indicating good binding activity (**Figure 6**). The network relationships of the above network pharmacology are shown in **Figure 5**.

Cell experiment results

The knockdown efficiency of three independent shRNAs targeting lncRNA GAS5 was verified by qPCR. All three significantly reduced GAS5 expression compared with sh-NC (P < 0.001), with sh-GAS5-2# showing the highest efficiency (Supplementary Figure 1). After 24 h of stimulation with TNF-α (10 ng/mL), the expression level of lncRNA GAS5 in MH7A cells was significantly lower than that in the normal control group. Co-treatment with GSZD (1,000 μg/mL) significantly reversed this downregulation, leading to increased lncRNA GAS5 expression (P < 0.001, **Figure 7**). In MH7A cells with stable knockdown of lncRNA GAS5, the effects of GSZD on TNF-α-induced cell viability (**Figure 8A**), apoptosis promotion (**Figure 8B**), and inhibition of PI3K/Akt phosphorylation (p-PI3K, p-Akt, **Figure 8C**) were all significantly reversed. Compared with the GSZD + TNF-α group, lncRNA GAS5 knockdown resulted in recovered cell viability, decreased apoptosis rate, and re-elevated p-PI3K and p-Akt levels (P < 0.05 or P < 0.01), confirming that lncRNA

Table 3. Comparison of TCM efficacy between the two groups after treatment

Group	Number of cases (n)	Clinical remission (n)	Marked improvement (n)	Effective (n)	Ineffective (n)	Total effective rate (%)
Control	30	0	0	6	24	20.0
Treatment	30	1	16	12	1	96.7
χ^2			40.16			
P value			< 0.0001			

Abbreviation: TCM, Traditional Chinese Medicine.

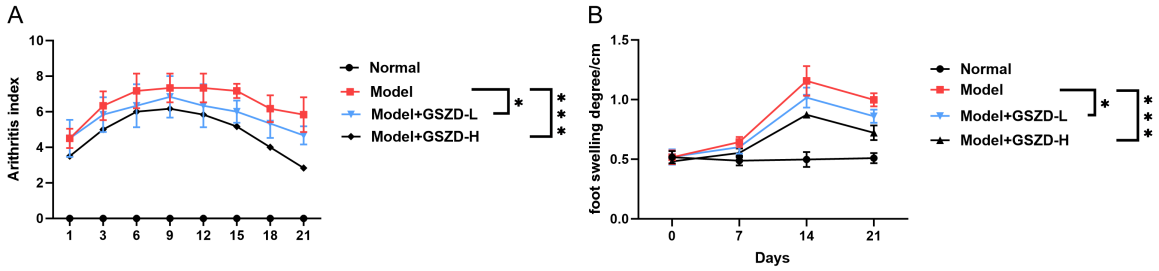


Figure 3. Joint inflammation in CIA rats: arthritis index (AI) scores and paw circumference. Rats were divided into four groups: Normal control, CIA model, GSZD low-dose, and GSZD high-dose. Data are presented as mean ± SD (n = 6 per group). $^{*}P < 0.05$; $^{***}P < 0.001$ vs. CIA model group. Abbreviation: GSZD, Guizhi-Shaoyao-Zhimu Decoction; CIA, collagen-induced arthritis; AI, arthritis index.

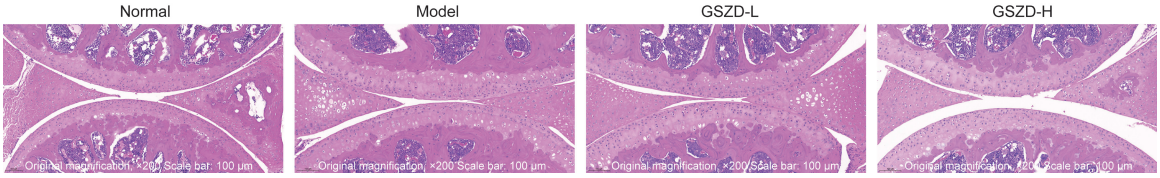


Figure 4. Representative histopathological changes of ankle joints in CIA rats after GSZD treatment (H&E staining). Four groups are shown: Normal control, CIA model, GSZD low-dose, and GSZD high-dose. Original magnification: ×200. Scale bar = 100 μm (n = 6 per group). Abbreviation: CIA, collagen-induced arthritis; GSZD, Guizhi-Shaoyao-Zhimu Decoction; H&E, hematoxylin and eosin.

Table 4. Active ingredients of GSZD retrieved from the TCMSP database

Herb	Number of active ingredients	
	Before screening (n)	After screening (n)
Guizhi	220	7
Baishao	85	13
Gancao	280	92
Mahuang	363	23
Shengjiang	265	5
Baizhu	55	7
Zhimu	81	15
Fangfeng	173	18
Fuzi	65	21

Abbreviation: GSZD, Guizhi-Shaoyao-Zhimu Decoction; TCMSP, Traditional Chinese Medicine Systems Pharmacology Database and Analysis Platform; OB, oral bioavailability; DL, drug-likeness.

GAS5 is a key mediator of the anti-RA effect of GSZD.

Discussion

This study systematically evaluated the therapeutic efficacy of GSZD in treating RA and its potential molecular mechanisms using clinical observation, animal experiments, network pharmacology, and cellular assays. The main findings are as follows: (1) GSZD combined with methotrexate (MTX) associated with improved clinical symptoms, reduced inflammatory indicators, and lower disease activity in RA patients, and the total effective rate was significantly higher than that with of MTX alone; (2) GSZD can dose-dependently alleviate joint inflammation and pathological damage in colla-

Table 5. Core target genes of GSZD in the treatment of rheumatoid arthritis

Gene symbol	Full name	Gene ID	Gene type
AKT1	AKT serine/threonine kinase 1	207	Protein-coding
IL6	interleukin 6	3569	Protein-coding
TNF	tumor necrosis factor	7124	Protein-coding
TP53	tumor protein p53	7157	Protein-coding
IL1B	interleukin 1 beta	3553	Protein-coding
PTGS2	prostaglandin-endoperoxide synthase 2	5743	Protein-coding
ESR1	estrogen receptor 1	2099	Protein-coding

Abbreviation: AKT1, AKT serine/threonine kinase 1; IL6, interleukin 6; TNF, tumor necrosis factor; TP53, tumor protein p53; IL1B, interleukin 1 beta; PTGS2, prostaglandin-endoperoxide synthase 2; ESR1, estrogen receptor 1.

gen-induced arthritis (CIA) rats; (3) Network pharmacology analysis suggests that the main active components of GSZD (quercetin, kaempferol, luteolin) may exert their effects through core targets such as AKT1, IL6, and TNF, and the PI3K/Akt signaling pathway is one of the important pathways; (4) Cell experiments confirmed that GSZD could reverse the downregulation of lncRNA GAS5 induced by TNF-α in MH7A cells and inhibit the phosphorylation activation of the PI3K/Akt signaling pathway by upregulating lncRNA GAS5, thereby inhibiting cell viability and promoting apoptosis; Knocking down lncRNA GAS5 can eliminate the effects of GSZD. These results reveal for the first time the epigenetic regulatory mechanism of GSZD in anti-RA from the perspective of the lncRNA GAS5/PI3K/Akt axis. Recent studies have further expanded the mechanistic understanding of GSZD in RA. Pang et al. demonstrated that GSZD alleviates synovial inflammation and bone erosion by blocking the IL-17R-MAPK cascade, with multiple GSZD components directly binding to IL-17R [9]. In addition, Zhang et al. reported that lncRNA GAS5 suppresses RA by inhibiting miR-361-5p and increasing PDK4 expression in FLS [10].

RA belongs to the category of “bi syndrome” in traditional Chinese medicine and is similar to “arthralgia”. Cold-dampness obstruction is one of the most common TCM patterns of RA. Its core pathogenesis involves insufficient yang qi, with cold-dampness invading the meridians and joints, leading to obstruction of qi and blood [11]. GSZD originates from the Jin Kui Yao Lue (Essential Prescriptions from the Golden Chamber). In this formula, Cinnamomi Ramulus (Guizhi) and Aconiti Lateralis Radix Praeparata (Fuzi) warm the meridians and dispel cold; Ephedrae Herba (Mahuang) and Saposhnikoviae Radix (Fangfeng) dispel wind and remove dampness; Atractylodis Macrocephalae Rhizoma (Baizhu) tonifies the spleen and dries dampness; Paeoniae Radix Alba (Baishao) and Anemarrhenae Rhizoma (Zhimu) nourish yin and clear heat; and Glycyrrhizae Radix et Rhizoma (Gancao) harmonizes the spleen and stomach. The entire formula uses both cold and hot elements and addresses both the symptoms and the root causes, precisely targeting the pathogenesis of cold-dampness obstruction combined with heat and yin injury. The results of this study show that after 12 weeks of treatment with GSZD in addition to MTX, the Chinese medicine symptom scores (joint tenderness, limited movement, cold sensation in the joints, aversion to wind and cold, cold extremities, soreness in the waist and knees, morning stiffness) of patients were significantly improved, and the total effective rate was as high as 96.7%, which was much higher than 20.0% in the MTX-alone group. This is consistent with previous clinical studies and Meta-analysis results, suggesting that GSZD may offer advantages in treating RA of the cold-dampness obstruction type [2].

In terms of conventional clinical indicators, the GSZD combined treatment group had significantly lower SJC, VAS, DAS28-ESR, DAS28-CRP, and serum TNF-α and IL-6 levels than the control group. This suggests that GSZD not only alleviates subjective symptoms of patients but also effectively inhibits systemic inflammatory responses. It is notable that DAS28 is the core indicator for evaluating RA disease activity, and its significant decrease indicates that GSZD helps achieve “targeted treatment”. Moreover, TNF-α and IL-6 are key drivers of synovial inflammation and joint destruction in

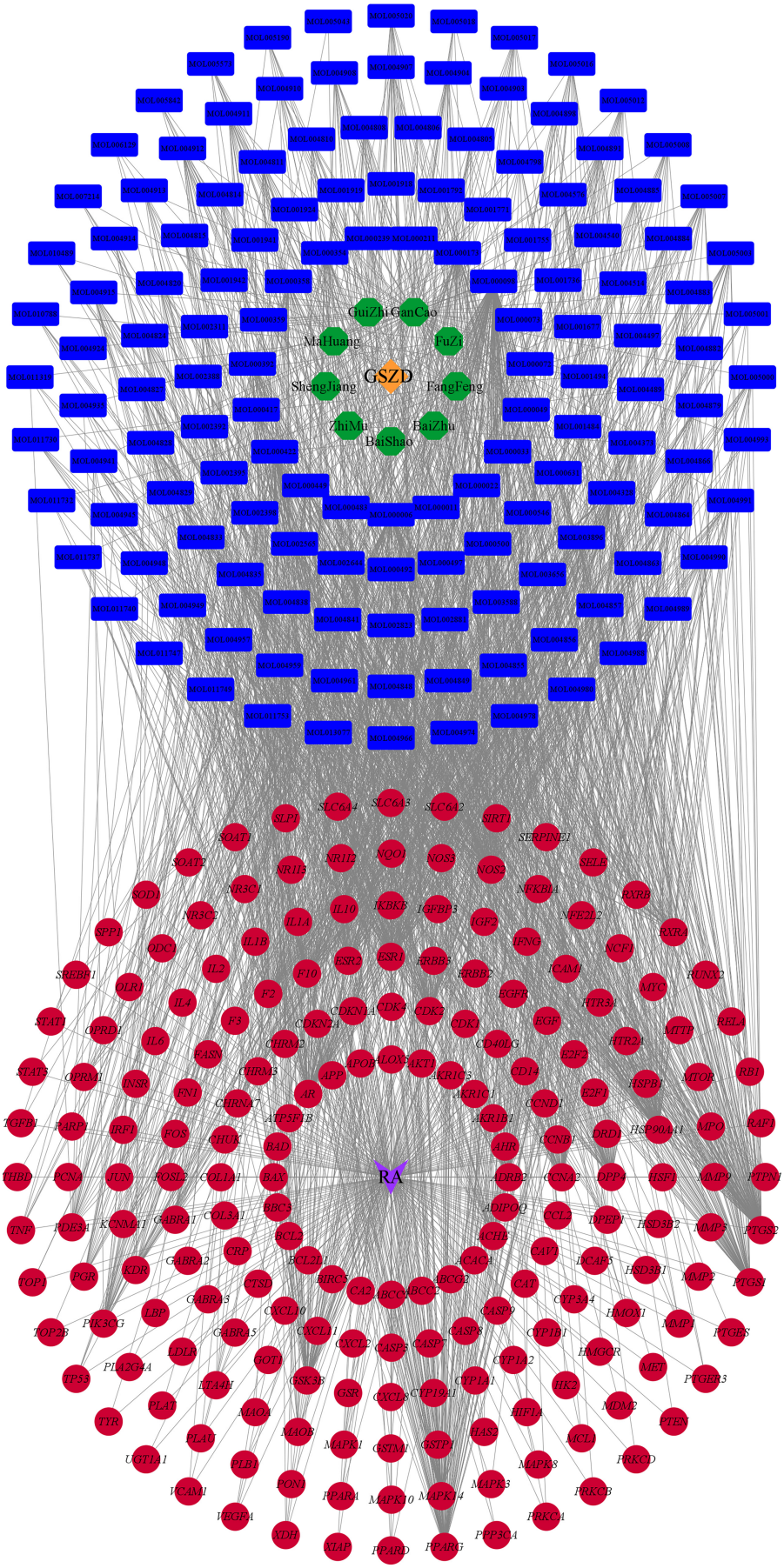

GuiZhiGanCao
MaHuang
FuZi
GSZD
ShangJiang
TangFeng
ZhiMu
BaiZhu
BaiShao
RA

Figure 5. Network pharmacology diagram: "GSZD-herb-active ingredient-target-RA" network. Abbreviation: GSZD, Guizhi-Shaoyao-Zhimu Decoction; RA, rheumatoid arthritis. Gene symbols and MOL IDs are labeled directly on the nodes. MOL IDs refer to the compound identifiers in the TCMSP database.

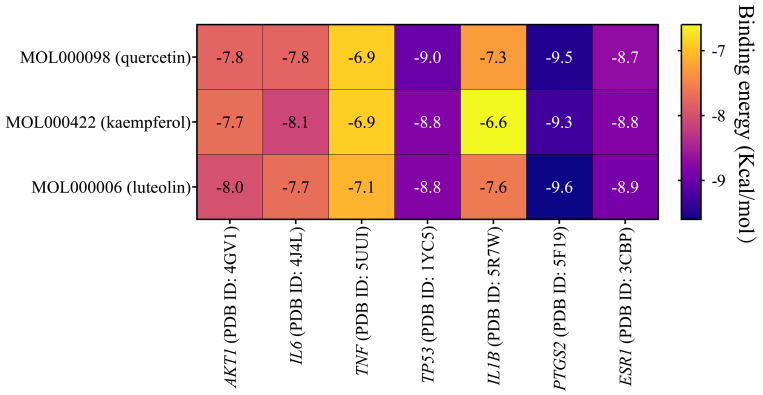


Figure 6. Molecular docking heatmap: binding energies of quercetin, kaempferol, and luteolin with core targets (AKT1, IL6, TNF, TP53, IL1B, PTGS2, ESR1). Abbreviation: AKT1, AKT serine/threonine kinase 1; IL6, interleukin 6; TNF, tumor necrosis factor; TP53, tumor protein p53; IL1B, interleukin 1 beta; PTGS2, prostaglandin-endoperoxide synthase 2; ESR1, estrogen receptor 1.

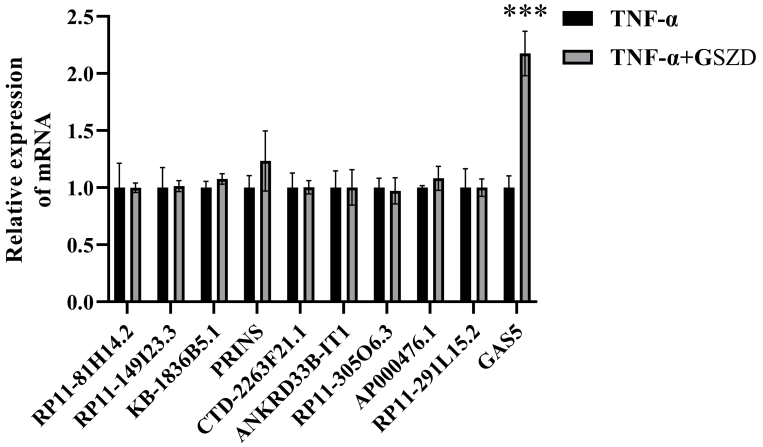


Figure 7. GSZD reverses TNF-α-induced downregulation of lncRNA GAS5 expression in MH7A cells. Data are presented as mean ± SD from three independent experiments. ***P < 0.001 vs. TNF-α group. Abbreviation: GSZD, Guizhi-Shaoyao-Zhimu Decoction; TNF-α, tumor necrosis factor-α; lncRNA GAS5, long non-coding RNA growth arrest-specific transcript 5; SD, standard deviation.

RA [12], and the inhibitory effect of GSZD on them provides direct evidence for its anti-inflammatory mechanism.

The CIA rat model is the most commonly used animal model for studying RA, and its pathological features (synovial hyperplasia, inflammatory infiltration, pannus formation, and cartilage erosion) are highly similar to those of human RA. This study found that both the low and high-dose GSZD groups could significantly reduce the arthritis index and paw circumference of CIA rats, and the high-dose group had a better effect, showing a dose-dependent pattern. HE staining further confirmed that GSZD intervention could significantly reduce synovial hyperplasia, inflammatory cell infiltration, and erosion of the cartilage surface, and the joint structure of the high-dose group basically returned to normal. These results are consistent with the conclusions of Yang et al. [13], indicating that GSZD has good anti-inflammatory and joint protection effects. Moreover, the efficacy of GSZD in this study shows a clear dose-response relationship, providing experimental references for the rational selection of doses in clinical practice.

Notably, the total effective rate in the MTX-alone group was 20.0%, which appears relatively low compared with some previous reports. Several factors may contribute to this observation. First, the criteria for TCM efficacy assessment used in this study were relatively stringent, with an improvement rate of ≥ 20% defined as "effective", ≥ 50% as "marked improvement", and ≥ 70% as "clinical remission". Second, the enrolled patients had relatively high baseline disease activity (mean DAS28-ESR 5.89 ± 0.65 in the control group), and MTX monotherapy often requires longer than 12 weeks to achieve optimal response in patients with moderate-to-high disease activity

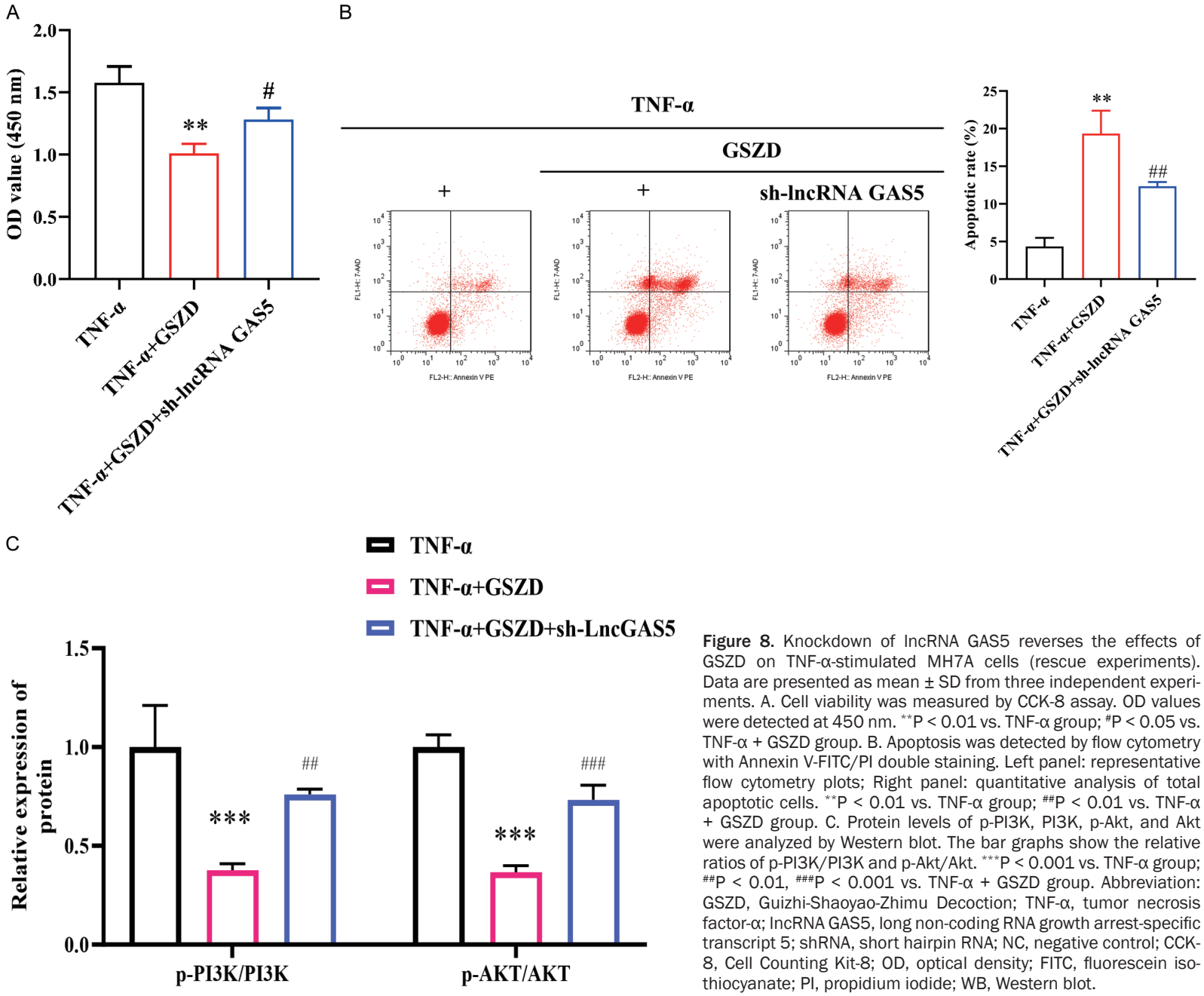


Figure 8. Knockdown of lncRNA GAS5 reverses the effects of GSZD on TNF-α-stimulated MH7A cells (rescue experiments). Data are presented as mean ± SD from three independent experiments. A. Cell viability was measured by CCK-8 assay. OD values were detected at 450 nm. $^{**}P < 0.01$ vs. TNF-α group; $^{\#}P < 0.05$ vs. TNF-α + GSZD group. B. Apoptosis was detected by flow cytometry with Annexin V-FITC/PI double staining. Left panel: representative flow cytometry plots; Right panel: quantitative analysis of total apoptotic cells. $^{**}P < 0.01$ vs. TNF-α group; $^{\#\#}P < 0.01$ vs. TNF-α + GSZD group. C. Protein levels of p-PI3K, PI3K, p-Akt, and Akt were analyzed by Western blot. The bar graphs show the relative ratios of p-PI3K/PI3K and p-Akt/Akt. $^{***}P < 0.001$ vs. TNF-α group; $^{\#\#}P < 0.01$, $^{\#\#\#}P < 0.001$ vs. TNF-α + GSZD group. Abbreviation: GSZD, Guizhi-Shaoyao-Zhimu Decoction; TNF-α, tumor necrosis factor-α; lncRNA GAS5, long non-coding RNA growth arrest-specific transcript 5; shRNA, short hairpin RNA; NC, negative control; CCK-8, Cell Counting Kit-8; OD, optical density; FITC, fluorescein isothiocyanate; PI, propidium iodide; WB, Western blot.

[2]. Third, real-world retrospective studies typically report lower response rates than strictly controlled randomized trials due to differences in patient selection, adherence, and confounding factors. Notably, a previous meta-analysis demonstrated that GSZD combined with conventional therapy significantly improved the total effective rate compared with MTX alone (RR = 1.17) [14], which is consistent with the superior efficacy of the GSZD-containing regimen observed in the present study.

Network pharmacology analysis revealed that after screening with OB ≥ 30% and DL ≥ 0.18, 201 active components were obtained from GSZD, among which quercetin, kaempferol, and luteolin were the components with the highest values. These three flavonoids have been shown to possess anti-inflammatory, antioxidant, immunomodulatory, and FLS-proliferation-inhibitory activities [3, 14, 15]. Quercetin can induce RA-FLS apoptosis by inhibiting the PI3K/Akt/mTOR pathway [16]; kaempferol can block the MAPK pathway to alleviate inflammation [17]; and luteolin can downregulate the activation of NLRP3 inflammasome [18]. The synergistic effect of these components may be the material basis for the multi-target efficacy of GSZD.

The PPI network identified 7 core targets: AKT1, IL6, TNF, TP53, IL1B, PTGS2, and ESR1. Among them, AKT1 is the core kinase of the PI3K/Akt pathway, and its abnormal activation is closely related to the proliferation, migration, and anti-apoptosis of RA-FLS; IL6 and TNF are key cytokines in the RA inflammation network [12]; IL1B plays a leading role in bone erosion [12]; PTGS2 (COX-2) catalyzes prostaglandin synthesis and mediates joint pain and inflammation [12]; the dysregulation of TP53 is related to the "tumorous-like" proliferation of FLS [19]; ESR1 is related to the gender tendency and disease activity of RA [20]. These targets cover multiple aspects such as inflammation, immunity, bone metabolism, and cell apoptosis, reflecting the overall regulatory characteristics of GSZD as "multi-component - multi-target".

Molecular docking results showed that the binding energies of quercetin, kaempferol, and luteolin to the above core targets were all less than -5.0 kcal/mol, suggesting good binding affinity, further supporting the prediction results of network pharmacology.

Cell experiments were the core mechanism verification part of this study. Firstly, we confirmed that TNF-α stimulation could significantly downregulate the expression of lncRNA GAS5 in MH7A cells, which is consistent with the clinical phenomenon of low expression of lncRNA GAS5 in RA patients [21, 22]. However, GSZD intervention could significantly reverse this downregulation, indicating that GSZD may counteract the activation effect of the inflammatory microenvironment on FLS by restoring the expression of lncRNA GAS5.

LncRNA GAS5 is a lncRNA with extensive regulatory functions, playing a role in tumor suppression or anti-inflammation in various diseases [7]. In RA, lncRNA GAS5 can sponge miR-222-3p to upregulate Sirt1 through the ceRNA mechanism, thereby inhibiting the proliferation of FLS and the release of inflammatory factors; it can also inhibit the AKT/mTOR pathway through the miR-128-3p/HDAC4 axis. This study provided reverse verification from the perspective of loss-of-function: in stable knockdown MH7A cells of lncRNA GAS5, the inhibitory effects of GSZD on the increase in cell viability, apoptosis inhibition, and inhibition of PI3K/Akt pathway phosphorylation induced by TNF-α were significantly reversed. These results directly prove that lncRNA GAS5 is a key mediator molecule for the anti-RA effect of GSZD, and its effect is at least partially achieved by regulating the PI3K/Akt signaling pathway. The PI3K/Akt pathway is a core regulatory hub for cell proliferation, survival, and metabolism. In RA-FLS, various inflammatory factors (such as TNF-α and IL-1β) can activate this pathway, leading to the acquisition of an invasive phenotype by FLS, resistance to apoptosis, and secretion of large amounts of MMPs to destroy cartilage. In this study, GSZD can significantly inhibit the levels of p-PI3K and p-Akt, and the inhibitory effect disappears after knockdown of lncRNA GAS5. Although PTEN was not measured, our data clearly show that GSZD significantly suppressed TNF-α-induced PI3K/Akt phosphorylation, and this suppression was largely reversed by lncRNA GAS5 knockdown.

The innovation of this study mainly lies in the following aspects: First, it directly links the anti-RA effect of the classic formula GSZD with the epigenetic regulator lncRNA GAS5, providing a new perspective for the mechanism study of

traditional Chinese medicine compound; Second, it adopts a multi-level verification strategy of "clinical-animal-network pharmacology-cell", forming a complete evidence chain from the whole to the molecular level; Third, the shRNA knockdown experiment reversely verified the necessity of lncRNA GAS5, enhancing the reliability of causal inference.

This study also has certain limitations. First, the clinical study was a retrospective cohort analysis with a small sample size (n = 30 per group) and without randomized assignment. Additionally, as the clinical data were retrospectively collected from routine practice without prospective trial registration, this limitation should be considered when interpreting the findings. This design inherently limits causal inference, and the observed associations between GSZD use and improved outcomes should be interpreted with caution. Although the two groups were comparable at baseline, potential confounding factors cannot be entirely excluded. Therefore, large-sample, multicenter, prospective randomized controlled trials are warranted to confirm these findings. Secondly, in the animal experiment, the protein expression of lncRNA GAS5 and the PI3K/Akt pathway in synovial tissue was not detected, and the role of this axis in vivo could not be directly verified. Thirdly, the cell experiment only used the MH7A cell line, which is widely used in RA-FLS research, but its biological behavior still differs from that of primary human FLS. Further verification in primary cells should be conducted. Fourthly, this study did not deeply explore the specific molecular mechanism of lncRNA GAS5 regulating the PI3K/Akt pathway (such as whether it is a ceRNA mechanism, whether it directly binds to Akt or other signaling proteins, etc.), nor did it identify the key active monomers regulating the expression of lncRNA GAS5 in GSZD. Finally, Western blot detected p-PI3K and p-Akt, but the detailed molecular mechanism by which lncRNA GAS5 regulates PI3K/Akt phosphorylation remains to be further investigated.

Conclusion

In conclusion, this study indicates that GSZD improves clinical symptoms and reduces inflammation in RA patients, and alleviates the joint inflammation and pathological damage in CIA rats. The mechanism is closely related to the upregulation of lncRNA GAS5 expression, which in turn inhibits the abnormal activation of the PI3K/Akt signaling pathway. These findings provide new molecular pharmacological evidence for the clinical application of GSZD and suggest that lncRNA GAS5 may become a potential epigenetic target for the treatment of RA. Future research should focus on: (1) Verifying the long-term efficacy and safety of GSZD in larger sample randomized controlled trials; (2) Isolating and identifying the key active components in GSZD that regulate lncRNA GAS5; (3) Deeply exploring the specific molecular regulatory network of lncRNA GAS5 in RA-FLS (such as ceRNA, RNA-protein interactions, etc.); and (4) Exploring the effects of GSZD on other immune cells (such as macrophages, T cells) in the lncRNA GAS5/PI3K/Akt axis to comprehensively understand its immunoregulatory function.

Disclosure of conflict of interest

None.

Address correspondence to: Zhenbin Li, Department of Rheumatology and Clinical Immunology, No. 980 Hospital of the Joint Logistics Support Force, The First Clinical Medical College of Nanjing University of Chinese Medicine, No. 398, Zhongshan West Road, Shijiazhuang 050000, Hebei, China. Tel: +86-0311-87978404; E-mail: lizb196-289@163.com

References

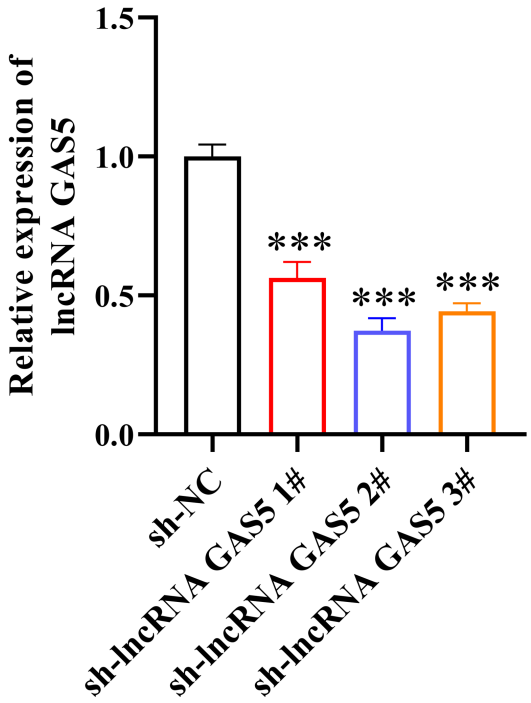
[1] Zhou W, Yang Y and Su L. Development and validation of predictive factors influencing rheumatoid arthritis associated with interstitial lung disease. Clin Rheumatol 2025; 44: 601-613.

[2] Feng C, Chen R, Wang K, Wen C and Xu Z. Chinese traditional medicine (GuiZhi-ShaoYao-ZhiMu decoction) as an add-on medication to methotrexate for rheumatoid arthritis: a meta-analysis of randomized clinical trials. Ther Adv Chronic Dis 2021; 12: 2040622321993438.

[3] Pan D, Guo Y, Liu Y, Yang H, Gong Z, Du Y, Xu R, Gao L, Xu Q and Li N. Guizhi Shaoyao Zhimu Decoction alleviates rheumatoid arthritis by inhibiting inflammation by targeting SLPI. Phytomedicine 2025; 139: 156471.

[4] Tofigh R, Hosseinpourfeizi M, Safaralizadeh R, Ghoddusifar S and Baradaran B. Serum levels

of long non-coding RNAs NEAT1, GAS5, and GAPLINC altered in rheumatoid arthritis. Curr Rheumatol Rev 2024; 20: 182-190.
[5] Yang Z, Lin SD, Zhan F, Liu Y and Zhan YW. LncRNA GAS5 alleviates rheumatoid arthritis through regulating miR-222-3p/Sirt1 signalling axis. Autoimmunity 2021; 54: 13-22.
[6] Yang PD, Zhu KJ, Lin SM, Chen ZX, Liu MY, Liu QP, Lin CS, Chu CQ and Xu Q. Association between neutrophils and renal impairment of rheumatoid arthritis: a retrospective cross-sectional study. Immun Inflamm Dis 2021; 9: 1000-1008.
[7] Hassani SS, Farhadi E, Esmaeili SA, Mahmoudi M, Mahmoudi M, Afshari JT, Akhlaghi M and Jamshidi A. Deciphering the role of ERK and PI3K/Akt as crosstalk pathways between fibroblast-like synoviocytes and osteoclasts; novel therapeutic approach for rheumatoid arthritis. Mol Biol Rep 2025; 52: 662.
[8] Zheng S, Li Z, Wang J, Li Y, Leng X and Wang S. Study on HPLC fingerprint and chemical pattern recognition of Guizhi Shaoyao Zhimu granules. Proceedings of the 11th International Conference on Biomedical Engineering and Bioinformatics 2022.
[9] Pang J, Chen T, Shen H, Jiang W, Tan Y, Zhang Z, Xu J, Yang F, Liu L and Li Y. Guizhi-Shaoyao-Zhimu Decoction regulates the IL-17R-MAPK pathway to alleviate rheumatoid arthritis. J Ethnopharmacol 2026; 371: 122020.
[10] Zhang W, Li B, Xia N, Zhu L, Zhang Z, Ren Z, Zhang L, Xu P, Meng F, Feng L and Yang L. lncRNA GAS5 suppresses rheumatoid arthritis by inhibiting miR-361-5p and increasing PDK4. Biochem Biophys Res Commun 2021; 583: 7-13.
[11] Li G, Liu Y, Meng F, Xia Z, Wu X, Fang Y, Zhang C and Liu D. Tanshinone IIA promotes the apoptosis of fibroblast-like synoviocytes in rheumatoid arthritis by up-regulating lncRNA GAS5. Biosci Rep 2018; 38: BSR20180626.
[12] Wei SJ, Zhang Q, Xiang YJ, Peng LY, Peng W, Ren Q and Gao YX. Guizhi-Shaoyao-Zhimu decoction attenuates bone erosion in rats that have collagen-induced arthritis via modulating NF-κB signalling to suppress osteoclastogenesis. Pharm Biol 2021; 59: 262-274.
[13] Yang J, Zhang S, Liu J, Xin L and Cao S. Objective TCM syndrome differentiation in rheumatoid arthritis patients with cerebral infarction: the auxiliary diagnostic value of autoantibodies (anti-CCP IgG, AKA, and GPI) and hemoglobin. Medicine (Baltimore) 2026; 105: e47610.
[14] He X, Li R, He X, He F, Xiao Y, Chen X, Lai Y, Guo W, Liu P, Cai X, Yang X, Shu Y, Shao J, Chen Y, Chen D, Quan M, Wu J, Xian L, He J, Ren H, Chen Z, Zhong Z, Liu L and Pan H. Elucidation of the anti-arthritic mechanism of Guizhi-Shaoyao-Zhimu decoction by reshaping circadian rhythm. Pharmacol Res 2025; 216: 107787.
[15] Ye H, Wang H, Han B, Chen K, Wang X, Ma F, Cheng L, Zheng S, Zhao X, Zhu J, Li J and Hong M. Guizhi Shaoyao Zhimu decoction inhibits neutrophil extracellular traps formation to relieve rheumatoid arthritis via gut microbial outer membrane vesicles. Phytomedicine 2025; 136: 156254.
[16] Xu Y, Huang Z, Wu G, Jin F, Lin S, Zhang C, Zheng J, Liu W, Hou J and Lu YJ. Bioinformatic assay reveal the potential mechanism of Guizhi-Shaoyao-Zhimu decoction against rheumatoid arthritis and mild-to-moderate COVID-19. Comput Methods Programs Biomed 2023; 238: 107584.
[17] Shi M, Li X, Yuan M, Chen F, Xu L, Pan X, Lv B and Teng J. Evaluation of the effects of Guizhi Shaoyao Zhimu decoction on rheumatoid arthritis by ultrasound combined with electrophysiological examination. Curr Med Imaging 2024; 20: e15734056306597.
[18] Yao H, Xiang L, Huang Y, Tan J, Shen Y, Li F, Geng F, Liu W, Li X and Gao Y. Guizhi Shaoyao Zhimu granules attenuate bone destruction in mice with collagen-induced arthritis by promoting mitophagy of osteoclast precursors to inhibit osteoclastogenesis. Phytomedicine 2023; 118: 154967.
[19] Shen J, Chen Q, Yang G and He Y. Observation of the curative effect of Guizhi-Shaoyao-Zhimu decoction combined with methotrexate in the treatment of early rheumatoid arthritis based on ultrasonic evaluation: study protocol of a randomized, double-blind, controlled clinical trial. Trials 2021; 22: 764.
[20] Guo M, Wang Z and Wang C. Exploration the molecular mechanisms of Guizhi Shaoyao Zhimu Decoction (GSZD) in the treatment of rheumatoid arthritis via network pharmacology. Asian J Surg 2024; [Epub ahead of print].
[21] Li Y, Zhu Y, Qi X, Shen R and Zhang H. SMI-guided deep remission and TCM-assisted biologic De-intensification in rheumatoid arthritis: Yiqi-Jianpi-Tongluo combined with TNF-α inhibitors. Pak J Pharm Sci 2026; 39: 1367-1380.
[22] He S, Hu SS, Xie J, Zhang J, Geng H and Jia E. Clinical characteristics of peripheral neuropathy and risk factors in rheumatoid arthritis patients: a retrospective study. Medicine (Baltimore) 2026; 105: e47156.



Supplementary Figure 1. Knockdown efficiency of three shRNAs targeting lncRNA GAS5 in MH7A cells. Cells were transfected with sh-NC or sh-lncRNA GAS5 1#, sh-lncRNA GAS5 2#, sh-lncRNA GAS5 3# for 48 h, and lncRNA GAS5 expression was measured by qPCR. Data are presented as mean ± SD from three independent experiments. ***P < 0.001 vs. sh-NC group. Abbreviation: sh-NC, short hairpin RNA negative control; sh-lncRNA GAS5 1#, shRNA targeting lncRNA GAS5 #1; sh-lncRNA GAS5 2#, shRNA targeting lncRNA GAS5 #2; sh-lncRNA GAS5 3#, shRNA targeting lncRNA GAS5 #3; qPCR, quantitative real-time polymerase chain reaction; SD, standard deviation.